Molecular Microbiology (2010) 76(3), 634–647 ■
doi:10.1111/j.1365-2958.2010.07102.x
First published online 12 April 2010

Influence of the nucleoid and the early stages of DNA replication on positioning the division site in *Bacillus subtilis*

S. Moriya,[‡] R. A. Rashid,[†‡] C. D. Andrade Rodrigues[‡] and E. J. Harry*
Institute for the Biotechnology of Infectious Diseases, University of Technology, Sydney, NSW 2007, Australia.

Summary

Although division site positioning in rod-shaped bacteria is generally believed to occur through the combined effect of nucleoid occlusion and the Min system, several lines of evidence suggest the existence of additional mechanisms. Studies using outgrown spores of *Bacillus subtilis* have shown that inhibiting the early stages of DNA replication, leading up to assembly of the replisome at *oriC*, influences Z ring positioning. Here we examine whether Z ring formation at midcell under various conditions of DNA replication inhibition is solely the result of relief of nucleoid occlusion. We show that midcell Z rings form preferentially over unreplicated nucleoids that have a bilobed morphology (lowering DNA concentration at midcell), whereas acentral Z rings form beside a single-lobed nucleoid. Remarkably however, when the DnaB replication initiation protein is inactivated midcell Z rings never form over bilobed nucleoids. Relieving nucleoid occlusion by deleting *noc* increased midcell Z ring frequency for all situations of DNA replication inhibition, however not to the same extent, with the DnaB-inactivated strain having the lowest frequency of midcell Z rings. We propose an additional mechanism for Z ring positioning in which the division site becomes increasingly potentiated for Z ring formation as initiation of replication is progressively completed.

Introduction

Bacterial cell division involves the invagination of the cell envelope to form a septum. The first known event in this process is the polymerization of the tubulin-like protein, FtsZ, into a ring, called the Z ring, which is positioned very precisely within the cell. How the Z ring is spatially and temporally coordinated to ensure faithful propagation is an area of intense research and the subject of several recent reviews (Dajkovic and Lutkenhaus, 2006; Harry *et al*., 2006; Barak and Wilkinson, 2007; Haeusser and Levin, 2008; Adams and Errington, 2009).

Two inhibitory factors that influence division site positioning in rod-shaped bacteria such as *Bacillus subtilis* and *Escherichia coli* are the Min system and nucleoid occlusion. In *B. subtilis* the Min system is not required for the precise positioning of the Z ring at midcell (Migocki *et al*., 2002). Rather the primary role of the Min system appears to be to prevent septum formation at potential division sites at the nucleoid-free cell poles (Harry *et al*., 2006; Lutkenhaus, 2007). Nucleoid occlusion prevents septum formation in the vicinity of the chromosome (Mulder and Woldringh, 1989; Woldringh *et al*., 1991; Harry *et al*., 2006). When chromosomes segregate, nucleoid occlusion is relieved between them to allow division in the midcell region of the cell (Woldringh *et al*., 1991; Yu and Margolin, 1999; Wu and Errington, 2004). Proteins responsible for nucleoid occlusion were recently identified: Noc (YyaA) in *B. subtilis* (Wu and Errington, 2004) and SlmA (Ttk) in *E. coli* (Bernhardt and de Boer, 2005). Both proteins associate with the chromosome and appear to act directly by preventing Z ring formation in this region of the cell (Wu and Errington, 2004; Bernhardt and de Boer, 2005; Wu *et al*., 2009). The Noc and SlmA proteins are not essential under normal growth conditions, but if chromosome replication or segregation is perturbed, they play a critical role in preventing guillotining of the DNA by the septum (Wu and Errington, 2004; Bernhardt and de Boer, 2005; Wu *et al*., 2009).

It is generally believed that precise positioning of the division site in rod-shaped bacteria arises from the combined action of nucleoid occlusion and the Min system (Wu and Errington, 2004; Bernhardt and de Boer, 2005). Consistent with this belief, although both Min and nucleoid occlusion genes are not essential, division is severely defective in Noc$^-$ *B. subtilis* and SlmA$^-$ *E. coli* cells when the Min system is also inactive (Wu and Errington, 2004; Bernhardt and de Boer, 2005). However, as noted previously, Z ring positioning in these cells is still biased towards division sites (internucleoid positions) (Wu and Errington, 2004; Bernhardt and de Boer, 2005). Furthermore, when

Accepted 17 February, 2010. *For correspondence. E-mail liz.harry@uts.edu.au; Tel. (+61) 2 9514 4173; Fax (+61) 2 9514 8349. [†]Present address: Seattle Biomedical Research Institute, 307 Westlake Ave N, Seattle, WA 98109, USA. [‡]These authors contributed equally to this work.

FtsZ is overproduced in *minD noc* double mutants of *B. subtilis*, a substantial number of Z rings form at internucleoid positions (Wu and Errington, 2004). These data strongly suggest that mechanisms in addition to nucleoid occlusion and Min regulate Z ring positioning in rod-shaped bacteria. Many bacteria do not have Min or Noc/SlmA, so other mechanisms must exist in these organisms to position the division site (Margolin, 2001).

A link between the very early stages of DNA replication and Z ring positioning in *B. subtilis* was established using outgrown spores (Harry *et al*., 1999; Regamey *et al*., 2000). This allowed inhibition of the first round of DNA replication at various stages leading up to assembly of the replisome at *oriC*, and examination of the effect on Z ring positioning. When the initiation phase of replication was blocked using a temperature sensitive *dnaB* mutation (*dna-1*), essentially all Z rings were positioned acentrally, to one side of the centrally located, unreplicated nucleoid (Harry *et al*., 1999). Similarly, when initiation of replication was permitted but DNA synthesis blocked using the DNA polymerase III inhibitor, HPUra [6-(para-hydroxyphenylazo)-uracil], the majority of Z rings were positioned acentrally (Regamey *et al*., 2000). Interestingly however, blocking chain elongation specifically by thymine starvation resulted in precise positioning of a substantial number of Z rings at midcell over the unreplicated nucleoid (Harry *et al*., 1999; Regamey *et al*., 2000).

Previously, the possibility was raised that degradation of the *oriC* region that occurs specifically under the thymineless conditions allows midcell Z ring assembly (Regamey *et al*., 2000). However, this is unlikely for two reasons. First, degradation of this region of the chromosome does not occur when midcell Z rings form under other conditions of a complete block to DNA synthesis (for example by addition of 0.03 μg ml^{-1} thymine; see Regamey *et al*., 2000). Second, while no degradation of the *oriC* region was detected when HPUra was added, a significant number of Z rings form at midcell when the nucleoid is centrally located and bilobed.

Here we show that differences in Z ring positioning as a result of early chromosome replication inhibition are not solely a consequence of different nucleoid occlusion effects. Rather, we propose that midcell Z ring assembly and the early stages of DNA replication are linked by a mechanism that acts in addition to nucleoid occlusion, such that the midcell region becomes increasingly 'potentiated' for Z ring assembly as the initiation phase of chromosome replication is progressively completed.

Results

The DNA replication initiation mutation, dnaF133*, allows Z ring assembly at midcell*

To examine the nature of the link between the early stages of DNA replication and division site positioning, we first tested whether Z rings could be positioned precisely at midcell in DNA replication inhibition situations other than the thymineless one. Accordingly, we found that the *dnaF133* mutation at the non-permissive temperature did allow a significant number of midcell Z rings to assemble in outgrown spores. *dnaF133* is a DNA initiation mutation that resides in the *polC* gene encoding the α-subunit of DNA polymerase III (Karamata and Gross, 1970; Attolini *et al*., 1976; Sanjanwala and Ganesan, 1991). This mutant showed a slow cut-off in DNA synthesis as expected for initiation mutants (Vrooman *et al*., 1978). Consistent with this interpretation, we confirmed that the Ori/Ter (*purA*/*metB*) marker ratio showed a decrease from 3.1 to 1.6 after 30 min at the non-permissive temperature (data not shown). Thus, the absence of significant ^{3}H-thymine incorporation into DNA after an early shift of germinated *dnaF133* spores to the non-permissive temperature (i.e. before the expected time of initiation of the first round) showed that initiation was completely blocked under such conditions (Table S1).

Using immunofluorescence we compared Z ring positioning in outgrown spores of the *dnaF133* mutant at the non-permissive temperature with another DNA initiation mutant, *dna-1*, which resides in the *dnaB* gene encoding a helicase co-loader (Winston and Sueoka, 1980; Velten *et al*., 2003; Rokop *et al*., 2004). [Note: *dnaB* of *B. subtilis* differs from *dnaB* of *E. coli*, which encodes a replicative helicase.] Z ring position is defined as the distance from the Z ring to the closest cell pole divided by the cell length, with 0.5 being exactly midcell. The vast majority of Z rings (78%) formed between positions 0.45 and 0.5 under wild-type conditions (SU8) at the non-permissive temperature (Fig. 1). As previously reported for *dna-1*, Z rings formed almost exclusively (92%) at acentral positions, alongside the centrally located nucleoid (Callister and Wake, 1977; Harry *et al*., 1999; Regamey *et al*., 2000). A similar result was observed for a different mutation in the *dnaB* gene, *dnaB19* (Imada *et al*., 1980) (data not shown). In contrast a significant proportion of the Z rings (32%) formed at midcell (0.45–0.5) in the *dnaF133* strain; fourfold more than *dna-1* (Fig. 1). The difference in Z ring positioning between the *dna-1* and *dnaF133* strains under non-permissive conditions is highly significant. The probability that the difference in midcell Z ring frequency between *dnaF133* and *dna-1* occurred by chance is only 0.003% (using the two-tailed Fisher's Exact test and a confidence interval of 0.05%). A summary of the Z ring positioning data, as well as the nucleoid morphology data, for all DNA replication inhibition conditions tested is provided in Table 1. A model that brings together all the data presented here is shown in Fig. 5, and can be referred to from this point.

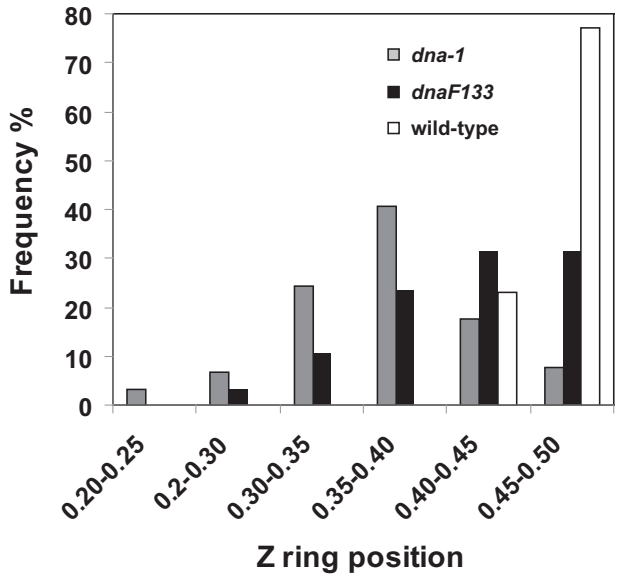

Fig. 1. Z ring positioning in *dna-1* and *dnaF133* at the non-permissive temperature. Spores were germinated at 34°C in PAB + T for 15–20 min prior to initiation of replication. They were then transferred to the non-permissive temperature (48°C) for 90 min and then fixed in methanol and prepared for immunofluorescence microscopy to visualize FtsZ. Mean cell lengths were 3.8 ± 0.08 μm (SEM) for SU472 (*dnaF133*) (black bars, $n = 124$), 4.5 ± 0.08 μm for SU46 (*dna-1*) (grey bars, $n = 91$) and 4.7 ± 0.06 μm for wild type (SU8; white bars, $n = 100$).

Nucleoid morphology differs between dnaF133 *and* dna-1 *mutants*

To determine whether the difference in Z ring positioning between *dnaF133* and *dna-1* cells is due to nucleoid occlusion effects, we examined nucleoids in live outgrown spores of these mutants at the non-permissive temperature using DAPI (6-diamidino-2-phenylindole). The nucleoids in all cases where DNA replication is inhibited are smaller than in wild-type outgrown cells due to continued cell elongation in the absence of DNA synthesis. Four types of nucleoid morphologies were observed and are shown in Fig. 2A. 'Single-lobed' nucleoids had one region of uniform staining, while 'bilobed' nucleoids consisted of two distinct regions of staining that were very close together. When two staining regions were well separated, the nucleoid was classified as 'separated', and when the nucleoid had more than two segments or was distributed between segments, it was classified as 'spread'. By far, the majority of nucleoids in *dna-1* at the non-permissive temperature consisted of single lobes (79%), with bilobes (16%), separated (3%) and spread (2%) accounting for the remaining nucleoids (Fig. 2B). In contrast, *dnaF133* had a much higher frequency of bilobes than *dna-1* (52%), and fewer single lobes (34%). Separated (11%) and spread (3%) nucleoids were a minor proportion of the population (Fig. 2C). Overall the bilobed nucleoids of the two strains looked similar (see Fig. S1 for various examples).

Examination of nucleoids in methanol-fixed cells confirmed our live cell observations. We observed similar appearances and frequencies of the four types of nucleoid morphologies in methanol-fixed *dna-1* and *danF133* cells (data not shown). We therefore conclude that there are genuine differences in the distribution of nucleoid morphologies between *dna-1* and *dnaF133* at the non-permissive temperature.

Midcell Z rings form preferentially over unreplicated bilobed nucleoids in dnaF133

We predicted that the majority of Z rings that were positioned at midcell would be present in cells that had bilobed nucleoids. Such nucleoids would presumably allow relief of nucleoid occlusion at midcell due to the lowered DNA concentration at this site. To test this prediction, the nucleoid and Z rings were co-visualized in live outgrown spores of *dna-1* and *dnaF133* at the non-permissive temperature. Z rings were visualized using a xylose-inducible *ftsZ–yfp* fusion integrated at the *amyE* locus of each strain to create *dna-1 ftsZ–yfp* (SU624) and *dnaF133 ftsZ–yfp* (SU625) respectively. As previously reported, growth and

Table 1. Summary of Z ring positioning[a] and unreplicated nucleoid morphology data.

Conditions of DNA replication inhibition	Midcell Z rings (%)[b]		Predominant nucleoid morphology[c]
	+noc	*Δnoc*	
Wild type	84	84	–[d]
DnaB mutation (*dna-1*, 48°C)	8	45	Single-lobed
PolC mutation (*dnaF133*, 48°C)	32	65	Bilobed
No thymine + HPUra (34°C)	22	75	Single-lobed
No thymine (34°C)	71	84	Bilobed

a. Z ring positioning was determined in fixed cells prepared for immunofluorescence.
b. Z ring position is measured as the ratio of the distance between the Z ring and the nearest cell pole divided by cell length. Between 0.45 and 0.5 is considered midcell.
c. Nucleoid morphologies observed in fixed cells. The distributions of nucleoid frequencies are similar between *+noc* and *Δnoc* strains.
d. Not determined. These cells have actively replicating nucleoids.

cell division were normal, and nucleoid morphology distributions were unchanged in the presence of 0.01% xylose (Migocki *et al*., 2002; Peters *et al*., 2007; Meredith *et al*., 2008). A similar proportion of total Z rings that were positioned at midcell were present in live cells of *dnaF133 ftsZ–yfp* and *dna-1 ftsZ–yfp* at the non-permissive temperature compared with those observed with immunofluorescence; 45% for *dnaF133* and 5% for *dna-1* (Fig. 2B and C respectively).

In both *dna-1* and *dnaF133* cells, when a single-lobed nucleoid is located at the cell centre, the Z ring preferentially forms to one side of it, in an acentral position (Fig. 2B, C, D-i and E-i). This was the most common phenotype in *dna-1*, representing 76% of all Z rings scored. In contrast, the majority of midcell Z rings in *dnaF133* formed over a centrally located, bilobed nucleoid (Fig. 2C and E-ii; Fig. S2E–H). Essentially the only time an acentral Z ring formed in a *dnaF133* cell with a bilobed nucleoid was when the nucleoid had moved off centre, such that one of the lobes was positioned at midcell.

Surprisingly, Z rings were never observed at midcell over bilobed nucleoids in the *dna-1* mutant at the non-permissive temperature, even though bilobed nucleoids represented 16% of the population (42 bilobes examined). When a centrally located bilobed nucleoid was present in this mutant, the Z ring still formed acentrally, even when the centre of the bilobe was at the centre of the cell (Fig. 2B and D-ii; Fig. S2A–D). Midcell Z rings only ever formed in *dna-1* when there was no observable DNA at the cell centre (see Fig. 2B).

The above data strongly suggest that Z rings can form at midcell more readily in *dnaF133* than *dna-1* cells regardless of apparent nucleoid occlusion effects. Two additional observations support this idea. First, we noticed an intriguing and statistically significant ($P < 0.05$) difference in Z ring positioning between the *dna-1* and *dnaF133* strains when DNA was physically absent from midcell (either because the nucleoid was well separated into two segments either side of midcell or because the nucleoid was positioned away from midcell). In these cases, *dnaF133* cells contained twice as many midcell Z rings (52%; 28 midcell rings out of 54 rings) compared with *dna-1* cells (26% midcell Z rings; 10 out of 39). Furthermore, a Z ring appeared to form over a substantial amount of DNA only in *dnaF133* cells, but not in *dna-1* cells. In four *dnaF133* cells, representing 1.6% of the total Z rings formed, a central Z ring formed over a central, single-lobed nucleoid (Fig. 2C and E-iii).

To rule out the possibility that nucleoid morphology changes after Z ring assembly, we examined Z rings and nucleoids at various times after germination. Germinated spores, including the wild-type and mutant strains used here, initially have a condensed single-lobed nucleoid (see also Ragkousi *et al*., 2000). Subsequently during outgrowth bilobed nucleoids appear. In both the *dna-1* and *dnaF133* strains, bilobed nucleoids were present prior to Z ring formation and the distribution of nucleoid morphologies was similar before and after Z ring assembly (data not shown), indicating that Z rings are positioned as a consequence of a particular nucleoid morphology, and not the other way around.

Central Z ring positioning correlates with a higher frequency of bilobed nucleoids under other conditions that block entry into the round of DNA replication

Our data show that when initiation of DNA replication is blocked, a central bilobed nucleoid allows a significant amount of midcell Z ring formation in the case of *dnaF133* but not *dna-1*. These results are consistent with the idea that Z rings form at midcell under two prerequisite conditions: (i) when the unreplicated nucleoid has adopted a bilobed conformation, and (ii) when some event linking the early stages of DNA replication and cell division has occurred. Based on condition (i), we predicted that other cases of DNA replication inhibition that allow midcell Z ring formation, such as the thymineless condition, would also have more bilobed nucleoids than single-lobed ones. On the other hand, withholding thymine but adding HPUra to also block DNA chain elongation, which gives rise to mainly acentral Z rings, should give rise to more single-lobed nucleoids (+HPUra condition; Harry *et al*., 1999).

We co-visualized nucleoids and Z rings in live outgrown thymine-requiring cells under both conditions at the permissive temperature of 34°C. The data presented are for the strain containing the *dna-1* mutation (SU624), and exactly the same results are obtained in the parent thymine-requiring strain that has a wild-type *dnaB* gene (SU8; Regamey *et al*., 2000). As predicted, we observed substantially more bilobed nucleoids under the thymineless condition (53%), compared with the +HPUra condition (10%), and significantly fewer single-lobed nucleoids (16%) than the +HPUra condition (56%) (Fig. 3A and B). All nucleoids in cells outgrown under the thymineless and +HPUra conditions occupied a larger volume of the cell compared with *dna-1* and *dnaF133* cells, and a higher proportion of nucleoids were present that contained more than two segments or that appeared stretched ('spread' morphology).

As reported previously, in the absence of thymine, the majority (71%) of Z rings were positioned at midcell, in contrast to the +HPUra case where proportion of Z rings that were positioned at midcell was much less frequent (22%; see Table 1). In both cases, cells with single-lobed nucleoids contained mainly acentral Z rings. Like *dnaF133* cells at the non-permissive temperature, under

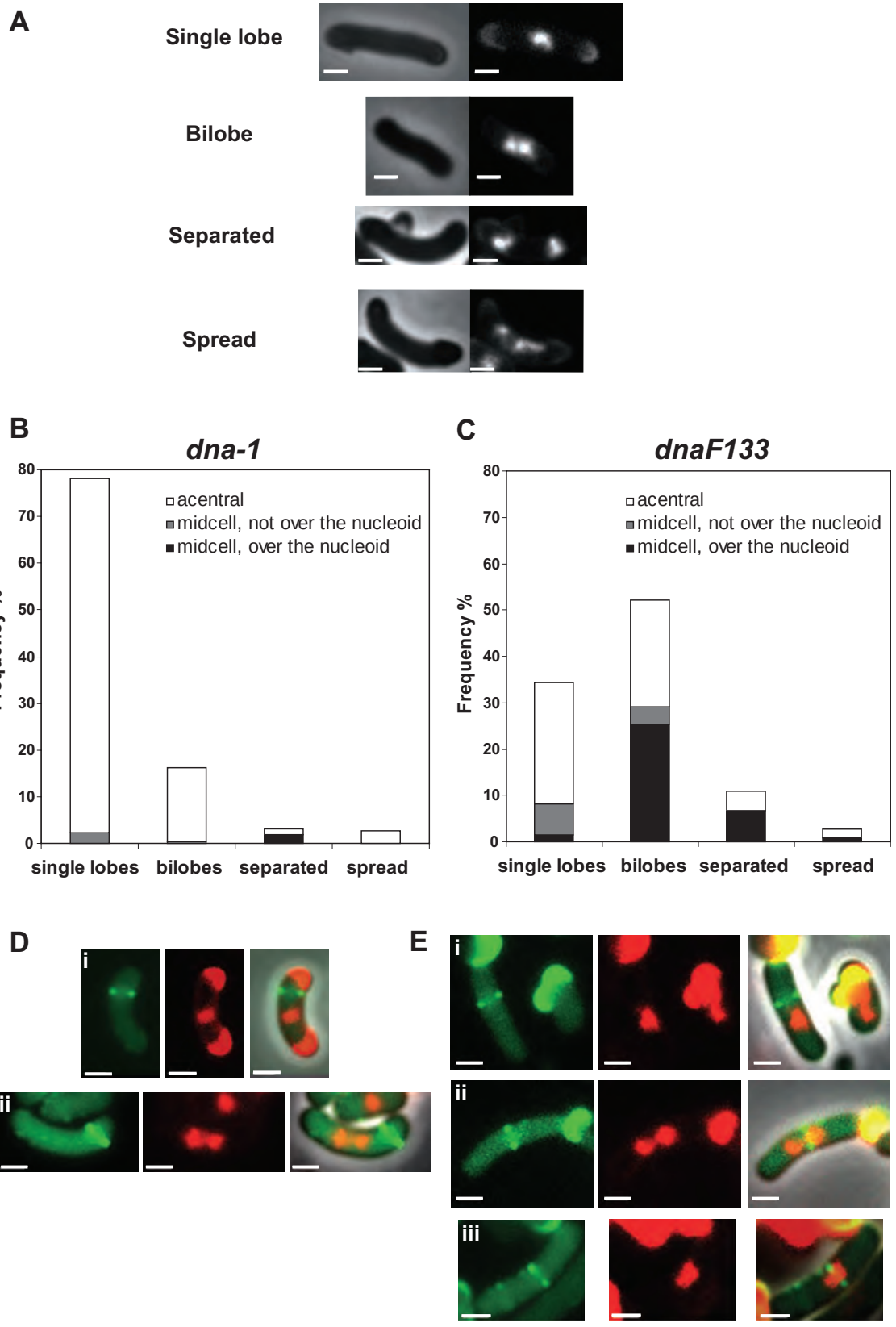
A
Single lobe
Bilobe
Separated
Spread
B
dna-1
Frequency %
acentral
midcell, not over the nucleoid
midcell, over the nucleoid
single lobes
bilobes
separated
spread
C
dnaF133
Frequency %
acentral
midcell, not over the nucleoid
midcell, over the nucleoid
single lobes
bilobes
separated
spread
D
i
ii
E
i
ii
iii

Fig. 2. Co-visualization of the Z ring and the nucleoid in *dna-1* and *dnaF133* at the non-permissive temperature.
A. The four types of nucleoid morphologies in live outgrown cells of SU472 (*dnaF133*) visualized by DAPI staining. SU46 (*dna-1*) outgrown cells had the same types. Spores were allowed to germinate at 34°C for 15–20 min prior to initiation of replication. They were then transferred to the non-permissive temperature (48°C) in PAB + T for 75 min. Mean cell lengths were 4.1 ± 0.06 μm (SEM) for SU46 and 4.0 ± 0.06 μm for SU472 ($n = 200$). Images shown are phase contrast (left) and DAPI (right). Autofluorescent spore coats can be seen in some fluorescent images. Scale bars are 1 μm.
B and C. Characterization of the Z ring with respect to the nucleoid in (B) SU624 (*dna-1 ftsZ–yfp*) and (C) SU625 (*dnaF133 ftsZ–yfp*). Spores were allowed to germinate at 34°C for 15–20 min prior to initiation of replication. They were then transferred to the non-permissive temperature (48°C) in PAB + T containing 0.01% xylose for 75 min. The height of each bar represents the frequency of each type of nucleoid morphology, showing the proportion of acentral Z rings (white), midcell Z rings over the nucleoid (black) and midcell Z rings that are not over the nucleoid (grey). Mean cell lengths were 4.61 ± 0.06 μm (SEM) for SU624 ($n = 260$) and 4.14 ± 0.04 μm for SU625 ($n = 257$).
D and E. Representative images of Z rings and nucleoids in (D) SU624 (*dna-1 ftsZ–yfp*) and (E) SU625 (*dnaF133 ftsZ–yfp*). SU624 (*dna-1 ftsZ–yfp*) cells show an acentral Z ring next to a centrally located single-lobed nucleoid (D-i) and an acentral Z ring next to a bilobed nucleoid (D-ii). SU625 (*dnaF33 ftsZ–yfp*) cells show an acentral Z ring next to a centrally located single-lobed nucleoid (E-i), a midcell Z ring over a bilobed nucleoid (E-ii) and a midcell Z ring over a single-lobed nucleoid (E-iii). Images shown are YFP pseudocoloured in green (left), DAPI pseudocoloured in red (middle) and overlay (right). Scale bars are 1 μm.

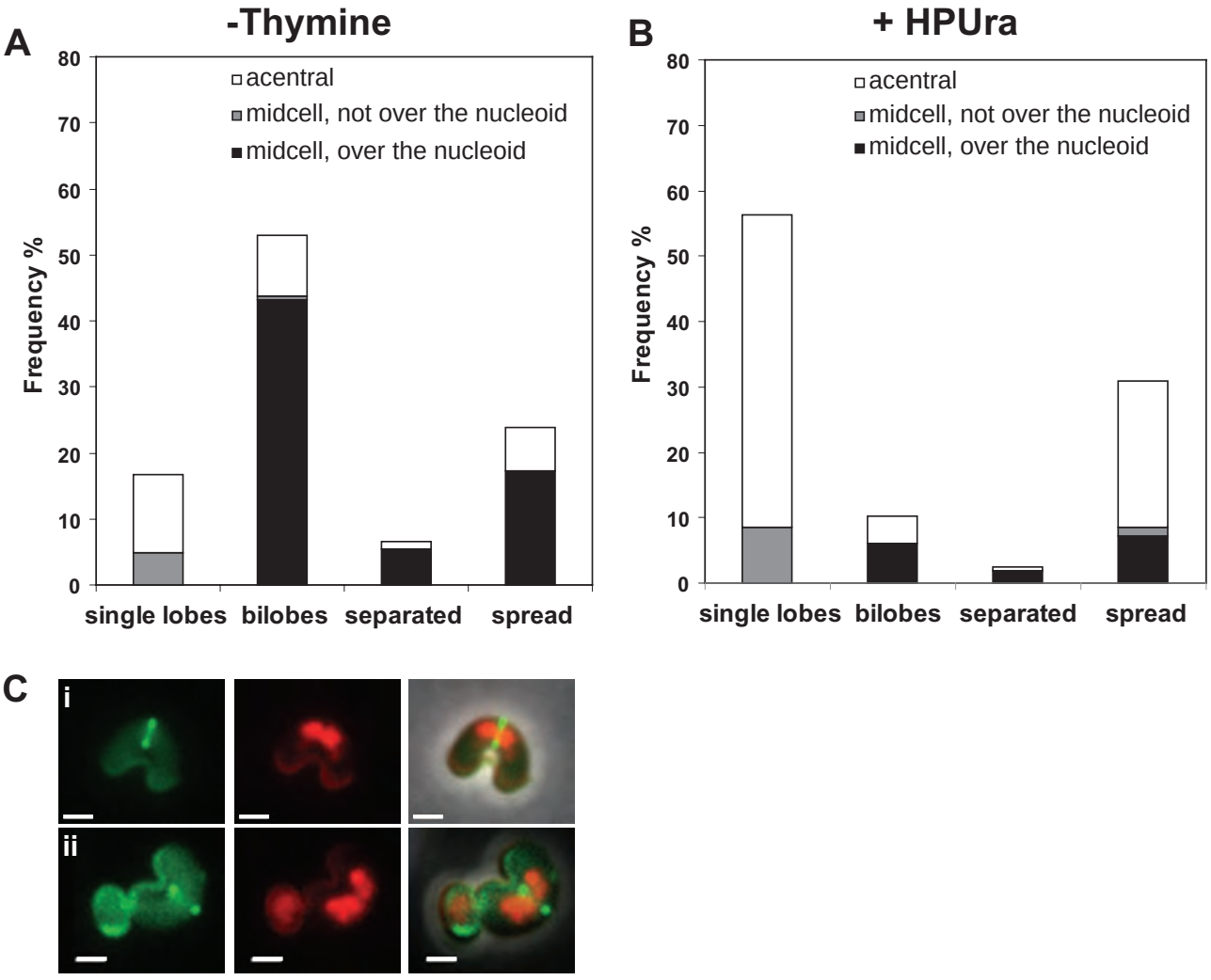

Fig. 3. Co-visualization of the Z ring and nucleoid under thymineless conditions and HPUra treatment.
A and B. SU624 (*dna-1, ftsZ–yfp*) spores were outgrown at 34°C in GMD with 0.01% xylose either lacking thymine (–thymine, $n = 185$) or lacking thymine with addition of 100 μM HPUra (+HPUra, $n = 165$). The height of each bar represents the frequency of each type of nucleoid morphology, showing the proportion of acentral Z rings (white), midcell Z rings over the nucleoid (black) and midcell Z rings that are not over the nucleoid (grey).
C. Representative images of a bilobed nucleoid and the Z ring in live outgrown spores of SU624 (*dna-1 ftsZ–yfp*) outgrown in the above described conditions: (i) no added thymine, and (ii) no thymine, 100 μM HPUra. Images shown are YFP pseudocoloured in green (left), DAPI pseudocoloured in red (middle) and overlay (right). Scale bars are 1 μm.

Table 2. *Bacillus subtilis* strains.

Strain	Description	Reference or source
1284	*trpC2 minD::pSG1737 (minCD'-lacZ ermC P_{spac}-min) Δnoc::tet*	Wu and Errington (2004)
L1436	*metC ilvA dnaF133*	L. Janniere
SU8 [SB566]	168 *thyA thyB trpC2*	A.T. Ganesan
SU46	*thyA thyB trpC2 dna-1*	N. Sueoka
SU434	SU8 *amyE::(spc P_{xyl}-ftsZ–yfp)*	Migocki *et al*. (2002)
SU472	SU8 *dnaF133*	This work
SU624	SU46 *amyE::(spc P_{xyl}-ftsZ–yfp)*	This work
SU625	SU472 *amyE::(spc P_{xyl}-ftsZ–yfp)*	This work
SU626	SU8 *Δnoc::tet*	This work
SU627	SU46 *Δnoc::tet*	This work
SU628	SU472 *Δnoc::tet*	This work
SU647	SU627 *amyE::(spc P_{xyl}-ftsZ–yfp)*	This work

Antibiotic genes are expressed as follows: *erm*, erythromycin; *tet*, tetracycline; *spc*, spectinomycin.

the thymineless conditions the majority of midcell Z rings formed over bilobed nucleoids, such that the Z ring formed at the centre of the bilobe (Fig. 3A and C-i).

In striking contrast to the complete absence of midcell Z rings over bilobed nucleoids in *dna-1* cells at the non-permissive temperature, a Z ring could still form at midcell over a bilobe in the +HPUra situation (Fig. 3B and C-ii), even though bilobes represented a smaller proportion of the overall nucleoid population (< 10% compared with 16% for *dna-1*; compare Fig. 2B with Fig. 3B). More than half of the HPUra-treated cells with a bilobed nucleoid had a midcell Z ring. We conclude that when the early stages of DNA replication (initiation and entry into the round) are inhibited, midcell Z rings that do form tend to do so over bilobed nucleoids, even when there are few such nucleoids. The *dna-1* mutation remains the exception to this rule.

In the absence of Noc midcell Z ring frequency increases to varying degrees, depending on the type of DNA replication inhibition

The nucleoid occlusion protein, Noc, is known to influence Z ring positioning when DNA replication is inhibited (Wu and Errington, 2004). We therefore deleted *noc* and examined midcell Z ring frequency under the different conditions of DNA replication inhibition. If Noc is the only factor that is causing changes to Z ring positioning under these conditions, then a *noc* deletion should result in all Z rings being positioned at midcell in all cases.

We initially examined the *dna1* and *dnaF133* strains. We introduced a *noc::tet* deletion cassette into the *dna-1* and *dnaF133* strains to create *dna-1 Δnoc::tet* (SU627) and *dnaF133 Δnoc::tet* (SU628) and performed immunofluorescence to examine Z ring positioning. *noc* was also deleted in the parent strain (SU626 in Table 2). The data are shown in Fig. 4A and summarized in Table 1. As expected (Wu and Errington, 2004), the distribution of nucleoid morphologies was unchanged in Noc-deleted mutant cells. This is shown for the *dna-1* strain in Fig. 4C. As reported previously (Wu and Errington, 2004), Z ring positioning was normal in the parent *Δnoc::tet* strain with 84% Z rings forming at midcell (0.45–0.5 position; Fig. 4A). In *dna-1* cells at the non-permissive temperature, the *noc* deletion caused an increase in the frequency of midcell Z rings from 8% in the presence of *noc* to 45% in its absence (Fig. 4A). In the *dnaF133* strain, *noc* deletion caused an increase in frequency of midcell Z rings from 32% to 65% (Fig. 4A).

The results above demonstrate that Noc does prevent some midcell Z ring formation when the initiation of DNA replication is blocked. Importantly however, while the frequency of midcell Z rings increased significantly in both mutants when Noc is absent, the rescue is not complete, nor is the frequency of midcell Z ring assembly the same in these strains. In other words, even in the absence of Noc the *dna-1* strain is still less capable of forming a midcell Z ring than the *dnaF133* mutant at the non-permissive temperature. These data demonstrate that the difference in frequency of midcell Z rings in the *dna-1* and *dnaF133* mutants at the non-permissive temperature is not solely due to the Noc protein.

Since there are more midcell Z rings than bilobed nucleoids in the *dna-1* strain when Noc is absent, a substantial number of these rings must form over a single-lobed nucleoid. Co-visualization of the Z ring and nucleoid in a strain in which *ftsZ–yfp* had been moved into the *dna-1 Δnoc::tet* strain confirmed that this is the case, with 64% of the midcell Z rings forming over single-lobed nucleoids (Fig. 4C and D). These results strongly argue against another, Noc-independent nucleoid occlusion mechanism being responsible for preventing midcell Z ring formation in the *dna-1* mutant at the non-permissive temperature.

We also tested whether midcell Z ring assembly would increase in both the thymineless and +HPUra situations in

the absence of Noc. We performed immunofluorescence on thymine-requiring *dna-1* spores (SU46) at the permissive temperature (34°C). The same results were obtained with the parent strain that has a wild-type *dnaB* gene (SU8; data not shown). If thymine is included in the medium, Z ring positioning is the same as wild type (84% of Z rings are at midcell) regardless of the presence or absence of *noc*. In the absence of thymine this is reduced to 71% midcell Z rings (see earlier). However when *noc* is deleted, the frequency of midcell Z rings goes back up to wild-type levels (Fig. 4B; Table 1). Deletion of *noc* in the presence of HPUra also almost fully restores Z ring positioning to normal, i.e. from 22% in Noc$^+$ cells to 75% in Noc$^-$ cells (Fig. 4B; Table 1). Again nucleoid morphologies were unchanged under these conditions in *noc*-deleted cells (see Fig. 4E and F for HPUra-inhibited cells). Like the *dna-1* mutant at the non-permissive temperature, the majority of HPUra-inhibited Noc$^-$ cells have single-lobed nucleoids (compare Fig. 4C with Fig. 4E). However, the frequency of midcell Z rings in *noc*-deleted HPUra-inhibited cells is substantially higher (75% compared with 45%). Furthermore colocalization of Z rings (*ftsZ–yfp*) and nucleoids in the *noc*-deleted HPUra-inhibited cells showed that a significant proportion of midcell Z rings formed directly over single-lobed nucleoids (27%; Fig. 4E and F).

The above data demonstrate that deletion of *noc*, under all conditions of DNA replication inhibition tested, significantly increases the frequency of midcell Z rings. However, it does not always fully restore midcell Z ring frequency back to wild-type levels, nor does it always result in the same frequency of midcell Z rings. Rather the frequency of midcell Z rings in the absence of *noc* still depends on the type of block to DNA replication.

Taken together, these data demonstrate that midcell Z ring assembly is linked to the early stages of replication in a way that is not solely a result of changes in nucleoid occlusion or nucleoid morphology (as defined here).

Noc is fully active in both dna-1 *and* dnaF133 *at the non-permissive temperature*

It is still intriguing that in Noc$^+$ cells, midcell Z rings can still form over centrally located bilobes under all DNA replication inhibition conditions tested above except in the *dna-1* strain at the non-permissive temperature. One possible explanation for this is that the Noc protein is more effective in the *dna-1* mutant than the *dnaF133* mutant at the non-permissive temperature so that, even when bilobed nucleoids form in the *dna-1* mutant, midcell Z rings cannot form over them.

To test this, spores of the *dnaF133* and *dna-1* strains containing the *ftsZ–yfp* fusion were outgrown at the non-permissive temperature and treated with chloramphenicol to make all nucleoids condense to a single-lobed morphology. The addition of chloramphenicol to wild-type cells inhibits translation, resulting in a highly condensed nucleoid that has been shown to mediate nucleoid occlusion of Z rings (Sun and Margolin, 2004). Presumably this is due to the activity of Noc. If Noc is fully active in both mutants, all Z rings should be positioned acentrally, to one side of the nucleoid. Addition of chloramphenicol (5 μg ml^{-1}) 30 min after the shift to the non-permissive temperature yielded mainly (> 90%) single-lobed, highly condensed nucleoids in both strains ($n > 300$ for each strain, data not shown) and Z rings formed in 21% of each population of cells. The rate of cell length extension was slightly slower than normal under these conditions (see *Experimental procedures*). Co-visualization of FtsZ and the nucleoid showed that for both mutants all the Z rings were positioning acentrally, next to a centrally located single-lobed nucleoid ($n > 130$ for each strain). The absence of midcell Z ring formation over a single-lobed nucleoid for either strain in the presence of chloramphenicol demonstrates that Noc is fully effective in both strains.

Discussion

In wild-type *B. subtilis* and *E. coli* cells the Z ring assembles at midcell only when a significant proportion of the chromosome has been replicated. However, we now show that, in addition to the thymineless situation, midcell Z rings also form when the initiation phase of chromosome replication is blocked by inactivation of PolC. The thymineless condition is therefore not unique in allowing premature midcell Z ring formation, and these new data firmly establish that Z rings can form precisely at midcell even when there is no DNA synthesis.

We propose that in Noc+ cells, when midcell Z rings do form, they have an almost exclusive preference for forming over the bilobed unreplicated nucleoids because of the lower concentration of DNA at the centre of the cell between the two lobes. This would relieve some nucleoid occlusion despite Noc being fully active, and is supported by the shift from midcell Z rings to acentral Z rings in the *dnaF133* mutant at the non-permissive temperature when chloramphenicol treatment causes bilobed nucleoids to become single-lobed. Why do unreplicated chromosomes form bilobes? Such ‘doublet’ nucleoids have previously been observed in *B. subtilis dna-1* outgrown spores at the non-permissive temperature (McGinness and Wake, 1979). The authors speculated that the bilobed nucleoid contains two large domains, corresponding to the two arms, which fold in upon each other. When DNA replication is blocked and the cell continues to elongate, these domains are separated to form the doublet. Such transverse separation of the left and right chromosome arms has been more recently demonstrated in *E. coli* by Sher-

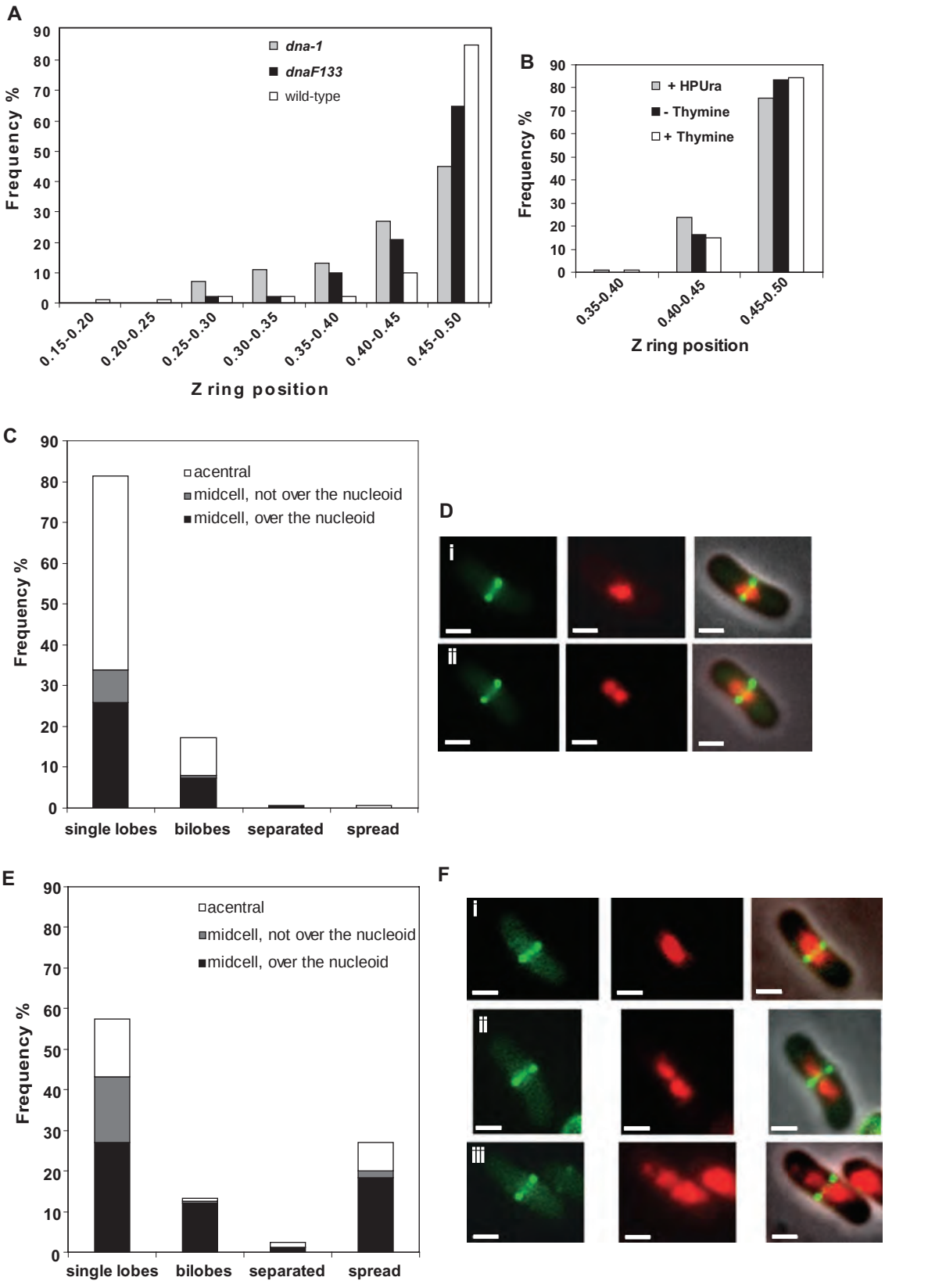
A
Frequency %
dna-1
dnaF133
wild-type
0.15-0.20
0.20-0.25
0.25-0.30
0.30-0.35
0.35-0.40
0.40-0.45
0.45-0.50
Z ring position
B
+ HPUra
- Thymine
+ Thymine
0.35-0.40
0.40-0.45
0.45-0.50
Z ring position
C
acentral
midcell, not over the nucleoid
midcell, over the nucleoid
single lobes
bilobes
separated
spread
D
i
ii
E
acentral
midcell, not over the nucleoid
midcell, over the nucleoid
single lobes
bilobes
separated
spread
F
i
ii
iii

Fig. 4. Z ring positioning in the absence of *noc*.
A. SU627 (*dna-1* Δ*noc::tet*), SU628 (*dnaF133* Δ*noc::tet*) and SU626 (SU8 Δ*noc::tet*) spores were germinated at 34°C for 15–20 min prior to initiation of replication. They were then transferred to the non-permissive temperature (48°C) in PAB + T for 90 min and then fixed in methanol and prepared for immunofluorescence microscopy to visualize FtsZ. The position of the Z ring was determined for SU627 (*dna-1* Δ*noc::tet*) (grey bars, $n > 200$), SU628 (*dnaF133* Δ*noc::tet*) (black bars, $n > 200$) and the wild-type strain SU626 (SU8 Δ*noc::tet*) (white bars, $n = 99$).
B. SU627 (*dna-1* Δ*noc::tet*) spores were outgrown in GMD at 34°C lacking thymine (–T, black bars) or also with 100 μM HPUra (–T +HPUra, grey bars), or with thymine (+T, white bars). Cells were collected at 180 min. Mean cell lengths were 3.87 ± 0.07 μm (SEM), 3.69 ± 0.06 μm and 4.27 ± 0.12 respectively ($n > 100$).
C and D. Co-visualization of the Z ring and nucleoid in SU647 (*dna-1*, Δ*noc::tet*, *ftsZ–yfp*). (C) Characterization of the Z ring with respect to the nucleoid in SU647 (*dna-1*, Δ*noc::tet*, *ftsZ–yfp*). Spores were allowed to germinate at 34°C for 15–20 min prior to initiation of replication. They were then transferred to the non-permissive temperature (48°C) in PAB + T containing 0.01% xylose for 75 min. The height of each bar represents the frequency of each type of nucleoid morphology, showing the proportion of acentral Z rings (white), midcell Z rings over the nucleoid (black) and midcell Z rings that are not over the nucleoid (grey). Mean cell lengths were 4.17 ± 0.04 μm (SEM) ($n = 162$). (D) Representative images of Z rings and nucleoids in SU647 (*dna-1*, Δ*noc::tet*, *ftsZ–yfp*) showing a midcell Z ring over a single-lobed nucleoid (D-i), and a midcell Z ring over a bilobed nucleoid (D-ii). Images shown are YFP pseudocoloured in green (left), DAPI pseudocoloured in red (middle) and overlay (right). Scale bars are 1 μm.
E and F. Co-visualization of the Z ring and nucleoid in HPUra-inhibited cells of SU647 (*dna-1*, Δ*noc::tet*, *ftsZ–yfp*). (E) Characterization of the Z ring with respect to the nucleoid in SU647 (*dna-1*, Δ*noc::tet*, *ftsZ–yfp*). Spores were outgrown in GMD at 34°C with 100 μM HPUra for 150 min. The height of each bar represents the frequency of each type of nucleoid morphology, showing the proportion of acentral Z rings (white), midcell Z rings over the nucleoid (black) and midcell Z rings that are not over the nucleoid (grey). Mean cell lengths were 4.01 ± 0.05 μm (SEM) ($n = 174$). (F) Representative images of Z rings and nucleoids in HPUra-inhibited SU647 (*dna-1*, Δ*noc::tet*, *ftsZ–yfp*) cells showing a midcell Z ring over a single-lobed nucleoid (F-i), a midcell Z ring over a bilobed nucleoid (F-ii) and a spread nucleoid (F-iii). Images shown are YFP pseudocoloured in green (left), DAPI pseudocoloured in red (middle) and overlay (right). Scale bars are 1 μm.

ratt and colleagues (Wang *et al*., 2006). We do not know why different treatments that block DNA replication give rise to different frequencies of nucleoid morphologies, particularly in the case of the thymineless and HPUra-treated cells, and this remains an interesting question.

Linking the early stages of DNA replication with midcell Z ring assembly: the 'ready-set-go' model

Our data demonstrate that differences in Z ring positioning as a consequence of inhibition of the early stages of DNA replication leading up to assembly of the replisome at *oriC* influence Z ring positioning in wild-type cells in a way that is not solely due to Noc activity. Furthermore, while it is possible that Noc-independent nucleoid occlusion mechanisms are present in *B. subtilis*, our observation that midcell Z rings form readily over single-lobed nucleoids in the absence of Noc strongly suggests that these mechanisms do not influence midcell Z ring assembly under prevention of the very early stages of DNA replication analysed here. Our nucleoid morphology data also raise the possibility that some aspect of chromosome organization affects Z ring positioning. For example, midcell Z ring assembly over the *dna-1* bilobes may be specifically prevented due to an alteration in chromosome organization.

Our observation that the frequency of midcell Z rings increases with progression of the initiation phase of replication in the absence of Noc leads us to propose a model for wild-type cells in which midcell becomes increasingly 'potentiated' for Z ring formation as initiation of DNA replication is progressively completed. This model is illustrated in Fig. 5. *dna-1* acts early in the initiation phase of replication after DnaA and DnaD (Velten *et al*., 2003; Smits *et al*., 2010), whereas the *dnaF133* mutation inactivates PolC, which assembles at *oriC* at the completion of initiation (Attolini *et al*., 1976; Love *et al*., 1976; Moriya *et al*., 1999). There is therefore less potentiation at midcell when DnaB is inactivated compared with PolC inactivation. The precise defect of *dnaF133* in DNA replication initiation is unknown, but at the non-permissive temperature PolC may not be loaded into the replisome (DNA replication machinery) at *oriC*. In the absence of thymine and with HPUra treatment, it is likely that DNA polymerase III is loaded into the replisome but is unable to proceed with DNA chain elongation. Consistent with this suggestion, we have observed a PolC-GFP focus in the midcell region of these cells (M. Migocki and E. Harry, unpubl. results). In these cases, there is maximum potentiation at midcell, and essentially a wild-type frequency of midcell Z ring in the absence of Noc. 'Potentiation' of midcell Z ring formation occurs possibly through maturation of a midcell site as previously proposed (Harry *et al*., 1999; Regamey *et al*., 2000; Migocki *et al*., 2004) or perhaps through the accumulation of a positive factor that contributes to midcell Z ring formation, as the cells prepare to enter the elongation stage of DNA replication. We favour this model over other possibilities because of our observation that midcell Z ring formation is progressively enhanced as the initiation phase of replication progresses. The ordered, stable association of replication initiation proteins with *oriC* in *B. subtilis* is consistent with this model (Smits *et al*., 2010).

This 'ready-set-go'-type mechanism predicts that DnaA is essential for midcell Z ring assembly (Moriya *et al*., 1999). Consistent with this idea, in the temperature sensitive (Noc$^+$) *dnaA1* mutant of *B. subtilis* (Moriya *et al*., 1990), the vast majority of Z rings are positioned acentrally in

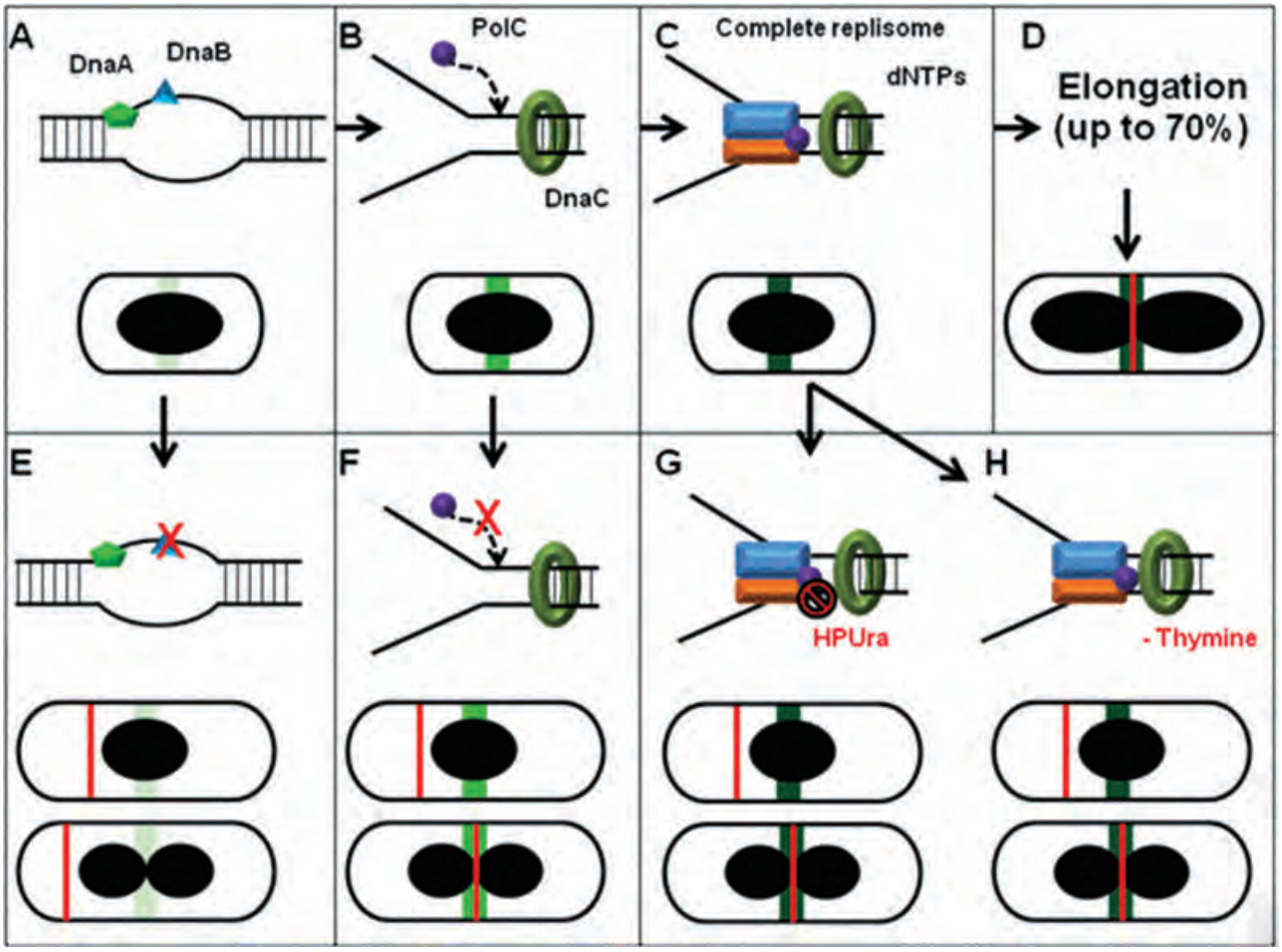

Fig. 5. Linking DNA replication with Z ring positioning: the 'ready-set-go' model.
A–D. During normal vegetative growth in *Bacillus subtilis*, early events of the initiation phase of DNA replication, leading up to the complete assembly of the replisome at *oriC*, promote the maturation of a midcell site. This possibly occurs through the accumulation of a positive factor for midcell Z ring formation at this site (increasing darkness of green shading). (A) The binding of the early initiation protein DnaA at *oriC* results in unwinding of DNA to trigger the start of the midcell 'potentiation'. Other early DNA replication initiation proteins, such as DnaB, then bind this region of the chromosome and increase midcell potentiation (light green area at midcell). (B) DnaC helicase is then loaded, followed by assembly of the components of the replisome at the newly formed replication fork. This includes PolC, the α-subunit of the replicative polymerase, and results in a further increase in potentiation at midcell (green area at midcell). (C) Recruitment and proper assembly of the remaining components of the replisome completes initiation and DNA synthesis is ready to occur. At this stage, midcell is 100% potentiated (dark green area at midcell) for Z ring formation (red line). (D) Midcell Z ring formation however only takes place once the bulk of replicating DNA and Noc are cleared from midcell. This would occur when significant replication of the chromosome (up to 70%) had occurred (Wu *et al*., 1995).
E–H. This lower panel shows what effect the various conditions of DNA replication inhibition have on (i) events occurring in the *oriC* region of the chromosome, (ii) the degree of potentiation at midcell and (iii) nucleoid morphology. (E) A block early in the initiation phase of DNA replication, such as inactivation of DnaB (as in the *dna-1* strain), would result in acentral Z ring formation because of the low potentiation level at midcell. Midcell Z rings do not form over bilobed nucleoids, as the amount of potentiation is not enough to overcome the nucleoid occlusion even when the nucleoid is bilobed. (F) A block at a later stage in DNA replication initiation, such as inactivation of PolC (as in the *dnaF133* strain), would result in more midcell potentiation and more midcell Z rings. This level of potentiation is high enough to allow a significant number of Z rings over bilobed nucleoids, despite some remaining nucleoid occlusion. (G and H) After initiation of replication is complete, but entry into the round (chain elongation) is inhibited, such as that resulting from the addition of HPUra (G) or the omission of thymine from the media (H), potentiation at midcell has already reached 100%. In these cases, the ability of the midcell Z ring to form is totally reliant on the level of nucleoid occlusion, dictated by the morphology of the nucleoid in this region. The only reason midcell Z rings are more frequent in the thymineless case compared with the HPUra one is that there are more bilobes in the former situation. For all cases described here (E–H) the single-lobed nucleoid prevents midcell Z ring formation even when potentiation levels are high.

outgrown cells at the non-permissive temperature (S. Moriya, unpubl. results). We did notice that a small number of these outgrown cells were able to replicate DNA at 48°C and formed midcell Z rings, presumably due to reversion or suppression of the *dnaA1* mutation. In *E. coli* cells harbouring the temperature sensitive *dnaA46* mutation, midcell Z ring formation over the nucleoid is blocked at the non-permissive temperature (Sun and Margolin, 2001).

oriC has been shown to localize to midcell prior to its replication (Lemon and Grossman, 1998; Regamey *et al*., 2000), so the initiation proteins are in an ideal location to play a role in midcell potentiation. Since Noc is not an essential protein in *B. subtilis* (Wu and Errington, 2004), our model predicts that in wild-type cells either another nucleoid occlusion protein or another mechanism blocks Z ring assembly at midcell at the start of DNA chain elongation (i.e. past the stages of DNA replication that we have inhibited here). The 'ready-set-go' model also predicts that the division site that is potentiated at midcell upon completion of initiation of replication remains potentiated until it is utilized when chromosome has been replicated beyond 70% completion (Wu *et al*., 1995).

Clearly, further studies are needed to clarify what regulates Z ring formation at midcell, and its relationship with the early stages of chromosome replication. This includes an analysis to establish conclusively what proteins are loaded at *oriC in vivo* under various DNA replication inhibition situations. The possibility that the effect on Z ring positioning observed here is a consequence of some aspect of chromosome orientation/structure cannot be ruled out and should also be tested.

Experimental procedures

Bacterial strains and growth conditions

Bacillus subtilis strains are listed in Table 1. SU472 (*dnaF133*) was obtained by congression of SU8 with DNA from strain L1436. To create SU625 (*dnaF133 ftsZ–yfp*), SU624 (*dna-1 ftsZ–yfp*) and SU647 (*dna-1, Δnoc::tet, ftsZ–yfp*) chromosomal DNA from SU434 (SU8 *ftsZ–yfp*) was used to transform SU472 (*dnaF133*), SU46 (*dna-1*) and SU627 (*dna-1 Δnoc::tet*). Spectinomycin-resistant colonies were selected and screened for temperature sensitivity, thymine auxotrophy and loss of amylase activity. To create SU626 (SU8 *Δnoc::tet*), SU627 (*dna-1 Δnoc::tet*) and SU628 (*dnaF133 Δnoc::tet*), chromosomal DNA from SU555 (strain 1284) (Wu and Errington, 2004) was transformed into SU8, SU46 (*dna-1*) or SU472 (*dnaF133*), and tetracycline-resistant colonies were selected. Temperature sensitivity of SU627 (*dna-1 Δnoc::tet*) and SU628 (*dnaF133 Δnoc::tet*) was confirmed.

Bacteria were grown vegetatively in PAB (antibiotic medium 3, Difco, USA) or TBAB (tryptose blood agar base, Difco, USA) at 30°C or 37°C. Thymine was added to a final concentration of 20 μg ml^{-1} unless otherwise indicated. Spectinomycin (60 μg ml^{-1}) or tetracycline (10 μg ml^{-1}) was added as applicable. To induce expression of *ftsZ–yfp*, 0.01% (w/v) xylose was included in the medium.

Spores were prepared and harvested as described previously (Migocki *et al*., 2004). Spore germination and outgrowth was performed with 2×10^8 spores ml^{-1} in GMD or PAB at 34°C (Harry *et al*., 1999; Regamey *et al*., 2000). Thymine was added to a final concentration of 20 μg ml^{-1} except for conditions of –T or –T +HPUra. Antibiotic selection was not applied during spore outgrowth. HPUra was added, where indicated, to a final concentration of 100 μM at the very beginning of the incubation. The time taken for spores to germinate varies between strains and is the reason why the time taken for outgrown cells to attain a certain length varies. However, the cell length of outgrown cells can be used as an indication of the stage of the cell cycle. For outgrowth at the non-permissive temperature, spores were germinated 15–20 min at 34°C with shaking and then transferred to 48°C for 75 or 90 min, with shaking. For outgrowth at the permissive temperature, spores were incubated at 34°C with shaking for the time indicated.

For the experiments with chloramphenicol, spores of SU624 (*dna-1 ftsZ–yfp*) and SU625 (*dnaF133 ftsZ–yfp*) were outgrown in PAB containing thymine for 20 min at 34°C and then transferred to 48°C for 90 min (SU624) or 105 min (SU625) to obtain an average cell length of 3.3 ± 0.04 μm (SEM) and 3.6 ± 0.05 μm respectively. Chloramphenicol (5 μg ml^{-1}) was added 30 min after the transfer to the non-permissive temperature. Co-visualization of the Z ring and nucleoid was performed as described below. For this experiment, 0.2% xylose was added to induce expression of *ftsZ–yfp*.

^{3}H-Thymidine incorporation

Thymidine incorporation assays were used to determine the ability of SU472 (*dnaF133*), SU46 (*dna-1*) and SU8 to replicate DNA at the non-permissive temperature in outgrown spores and in vegetatively growing cells. Spores were germinated and outgrown for 90 min at the non-permissive temperature as described above (including 20 μg ml^{-1} thymine) but with [methyl-^{3}H]thymidine (10 μCi, specific activity 80.9 Ci mmol^{-1}, American Radiolabeled Chemicals) included in the medium. Samples (0.5 ml) were taken over a time course and added to tubes containing 0.05 ml of 2 M NaOH. Samples were incubated 30 min at 80°C (to degrade RNA) and then 30 min on ice before addition of 5 ml of ice-cold 10% trichloroacetic acid (to precipitate DNA). The samples were collected on GF/C glass microfibre filters (25 mm diameter, Whatman, England) and washed twice with ice-cold 5% trichloroacetic acid. The filters were washed with 100% ethanol, dried at 60°C and covered with 10 ml of scintillation fluid (4 g of PPO per litre of Toluene). Radioactivity was measured in a Wallace 1409 liquid scintillation counter, and all samples were performed in triplicate. To determine if SU472 (*dnaF133*) has a defect in DNA replication initiation or chain elongation, the same procedure was used with cells grown vegetatively at 33°C and then transferred to the non-permissive temperature (48°C). Cells were monitored for 150 min following the temperature shift.

Fluorescence microscopy

Immunofluorescence microscopy was performed using affinity-purified rabbit anti-FtsZ antibodies (raised against *B. subtilis* FtsZ) and Alexa 488-conjugated secondary antibodies (Molecular Probes, Invitrogen, USA) as described previously (Peters *et al*., 2007). Live cells were visualized on 2% (w/v) agarose pads using Gene Frame (AB Genes) to create a flat surface on the glass slide. DAPI was added at a final

concentration of 0.4 μg ml^{-1} before placing the cells on the agarose pad. The same procedure was performed for co-visualization of the nucleoid and Z ring in live cells, with the addition of 0.01% (w/v) xylose included in the outgrowth medium to maintain expression of *ftsZ–yfp*. Approximately 80% and 40% of cells had a Z ring in live cell and immunofluorescence experiments respectively.

To examine nucleoids in fixed cells, bacteria were grown as for live cell visualization and 1 ml of culture was fixed in 10 ml of ice-cold methanol for 1 h, then washed in PBS and attached to a poly-L-lysine-treated glass slide. DAPI was added to 50% glycerol in PBS at a final concentration of 0.4 μg ml^{-1}, and this solution was added to the fixed cells just before placement of the coverslip.

All images were taken on a Zeiss Axioplan 2 fluorescence microscope equipped with a Plan ApoChromat (100×, NA 1.4; Zeiss) objective lens and an AxioCam MRm cooled CCD camera. The light source was a 100 W high-pressure mercury lamp passed through the following filters: for visualizing Alexa 488 (Filter set 09, Zeiss), for visualizing DAPI (Filter set 02, Zeiss; 365) and for visualizing YFP (Filter set 41029, Chroma Technology). Axio Vision software was used for image analysis (AxioVision LE v4.5, Carl Zeiss).

Measurement of Z ring positioning

Z ring position was determined by measuring the distance from the Z ring to the closest cell pole divided by the total cell length, with 0.5 being precisely midcell. A Z ring was considered to be at midcell if it was positioned within the range of 0.45–0.50, where essentially all Z rings formed in the parent background (SU8) under the same conditions.

Statistical analysis

The two-tailed Fisher's Exact test was used to compare the frequency of midcell Z ring formation in all cases, both in the presence and in the absence of *noc*. The *Z*-test was used to compare cell length measurements.

Acknowledgements

The authors gratefully acknowledge L. Jannière and J. Errington for the gift of strains. The authors wish to thank R.G. Wake for his valuable insights and R.G. Rashid for statistical advice. We also thank W. Burkholder and P.A.J. de Boer for critical reading of the manuscript. This research was supported by an Australian Research Council Discovery Project Grant (DP0666670) to E.J.H. and an Australian Postgraduate Award to C.D.A.R.

References

Adams, D.W., and Errington, J. (2009) Bacterial cell division: assembly, maintenance and disassembly of the Z ring. *Nat Rev Microbiol* **7:** 642–653.

Attolini, C., Mazza, G., Fortunato, A., Ciarrocchi, G., Mastromei, G., Riva, S., and Falaschi, A. (1976) On the identity of *dnaP* and *dnaF* genes of *Bacillus subtilis*. *Mol Gen Genet* **148:** 9–17.

Barak, I., and Wilkinson, A.J. (2007) Division site recognition in *Escherichia coli* and *Bacillus subtilis*. *FEMS Microbiol Rev* **31:** 311–326.

Bernhardt, T.G., and de Boer, P.A. (2005) SlmA, a nucleoid-associated, FtsZ binding protein required for blocking septal ring assembly over chromosomes in *E. coli*. *Mol Cell* **18:** 555–564.

Callister, H., and Wake, R.G. (1977) Completion of the replication and division cycle in temperature-sensitive DNA initiation mutants of *Bacillus subtilis* 168 at the non-permissive temperature. *J Mol Biol* **117:** 71–84.

Dajkovic, A., and Lutkenhaus, J. (2006) Z ring as executor of bacterial cell division. *J Mol Microbiol Biotechnol* **11:** 140–151.

Haeusser, D.P., and Levin, P.A. (2008) The great divide: coordinating cell cycle events during bacterial growth and division. *Curr Opin Microbiol* **11:** 94–99.

Harry, E.J., Rodwell, J., and Wake, R.G. (1999) Co-ordinating DNA replication with cell division in bacteria: a link between the early stages of a round of replication and mid-cell Z ring assembly. *Mol Microbiol* **33:** 33–40.

Harry, E., Monahan, L., and Thompson, L. (2006) Bacterial cell division: the mechanism and its precision. *Int Rev Cytol* **253:** 27–94.

Imada, S., Carroll, L.E., and Sueoka, N. (1980) Genetic mapping of a group of temperature-sensitive DNA initiation mutants in *Bacillus subtilis*. *Genet* **94:** 809–823.

Karamata, D., and Gross, J.D. (1970) Isolation and genetic analysis of temperature-sensitive mutants of *B. subtilis* defective in DNA synthesis. *Mol Gen Genet* **108:** 277–287.

Lemon, K.P., and Grossman, A.D. (1998) Localization of bacterial DNA polymerase: evidence for a factory model of replication. *Science* **282:** 1516–1519.

Love, E., D'Ambrosio, D., and Brown, N.C. (1976) Mapping of the gene specifying DNA polymerase III of *Bacillus subtilis*. *Mol Gen Genet* **144:** 313–321.

Lutkenhaus, J. (2007) Assembly dynamics of the bacterial MinCDE system and spatial regulation of the Z ring. *Annu Rev Biochem* **76:** 539–562.

McGinness, T., and Wake, R.G. (1979) Completed *Bacillus subtilis* nucleoid as a doublet structure. *J Bacteriol* **140:** 730–733.

Margolin, W. (2001) Spatial regulation of cytokinesis in bacteria. *Curr Opin Microbiol* **4:** 647–652.

Meredith, D.H., Plank, M., and Lewis, P.J. (2008) Different patterns of integral membrane protein localization during cell division in *Bacillus subtilis*. *Microbiology* **154:** 64–71.

Migocki, M.D., Freeman, M.K., Wake, R.G., and Harry, E.J. (2002) The Min system is not required for precise placement of the midcell Z ring in *Bacillus subtilis*. *EMBO Rep* **3:** 1163–1167.

Migocki, M.D., Lewis, P.J., Wake, R.G., and Harry, E.J. (2004) The midcell replication factory in *Bacillus subtilis* is highly mobile: implications for coordinating chromosome replication with other cell cycle events. *Mol Microbiol* **54:** 452–463.

Moriya, S., Kato, K., Yoshikawa, H., and Ogasawara, N. (1990) Isolation of a *dnaA* mutant of *Bacillus subtilis* defective in initiation of replication: amount of DnaA protein determines cells' initiation potential. *EMBO J* **9:** 2905–2910.

Moriya, S., Imai, Y., Hassan, A.K., and Ogasawara, N. (1999)

Regulation of initiation of *Bacillus subtilis* chromosome replication. *Plasmid* **41:** 17–29.
Mulder, E., and Woldringh, C.L. (1989) Actively replicating nucleoids influence positioning of division sites in *Escherichia coli* filaments forming cells lacking DNA. *J Bacteriol* **171:** 4303–4314.
Peters, P.C., Migocki, M.D., Thoni, C., and Harry, E.J. (2007) A new assembly pathway for the cytokinetic Z ring from a dynamic helical structure in vegetatively growing cells of *Bacillus subtilis*. *Mol Microbiol* **64:** 487–499.
Ragkousi, K., Cowan, A.E., Ross, M.A., and Setlow, P. (2000) Analysis of nucleoid morphology during germination and outgrowth of spores of *Bacillus* species. *J Bacteriol* **182:** 5556–5562.
Regamey, A., Harry, E.J., and Wake, R.G. (2000) Mid-cell Z ring assembly in the absence of entry into the elongation phase of the round of replication in bacteria: co-ordinating chromosome replication with cell division. *Mol Microbiol* **38:** 423–434.
Rokop, M.E., Auchtung, J.M., and Grossman, A.D. (2004) Control of DNA replication initiation by recruitment of an essential initiation protein to the membrane of *Bacillus subtilis*. *Mol Microbiol* **52:** 1757–1767.
Sanjanwala, B., and Ganesan, A.T. (1991) Genetic structure and domains of DNA polymerase III of *Bacillus subtilis*. *Mol Gen Genet* **226:** 467–472.
Smits, W.K., Goranov, A.I., and Grossman, A.D. (2010) Ordered association of helicase loader proteins with the *Bacillus subtilis* origin of replication *in vivo*. *Mol Microbiol* **75:** 452–461.
Sun, Q., and Margolin, W. (2001) Influence of the nucleoid on placement of FtsZ and MinE rings in *Escherichia coli*. *J Bacteriol* **183:** 1413–1422.
Sun, Q., and Margolin, W. (2004) Effects of perturbing nucleoid structure on nucleoid occlusion-mediated toporegulation of FtsZ ring assembly. *J Bacteriol* **186:** 3951–3959.
Velten, M., McGovern, S., Marsin, S., Ehrlich, S.D., Noirot, P., and Polard, P. (2003) A two-protein strategy for the functional loading of a cellular replicative DNA helicase. *Mol Cell* **11:** 1009–1020.
Vrooman, M.J., Barnes, M.H., and Brown, N.C. (1978) *Bacillus subtilis dnaF*: a mutation of the gene specifying the structure of DNA polymerase III. *Mol Gen Genet* **164:** 335–339.
Wang, X., Liu, X., Possoz, C., and Sherratt, D.J. (2006) The two *Escherichia coli* chromosome arms locate to separate cell halves. *Genes Dev* **20:** 1727–1731.
Winston, S., and Sueoka, N. (1980) DNA–membrane association is necessary for initiation of chromosomal and plasmid replication in *Bacillus subtilis*. *Proc Natl Acad Sci USA* **77:** 2834–2838.
Woldringh, C.L., Mulder, E., Huls, P.G., and Vischer, N. (1991) Toporegulation of bacterial division according to the nucleoid occlusion model. *Res Microbiol* **142:** 309–320.
Wu, L.J., and Errington, J. (2004) Coordination of cell division and chromosome segregation by a nucleoid occlusion protein in *Bacillus subtilis*. *Cell* **117:** 915–925.
Wu, L.J., Franks, A.H., and Wake, R.G. (1995) Replication through the terminus region of the *Bacillus subtilis* chromosome is not essential for the formation of a division septum that partitions the DNA. *J Bacteriol* **177:** 5711–5715.
Wu, L.J., Ishikawa, S., Kawai, Y., Oshima, T., Ogasawara, N., and Errington, J. (2009) Noc protein binds to specific DNA sequences to coordinate cell division with chromosome segregation. *EMBO J* **28:** 1940–1952.
Yu, X.C., and Margolin, W. (1999) FtsZ ring clusters in min and partition mutants: role of both the Min system and the nucleoid in regulating FtsZ ring localization. *Mol Microbiol* **32:** 315–326.

Supporting information

Additional Supporting Information may be found in the online version of this article:

Please note: Wiley-Blackwell are not responsible for the content or functionality of any supporting materials supplied by the authors. Any queries (other than missing material) should be directed to the corresponding author for the article.